Available online at www.sciencedirect.com
ScienceDirect
Trans. Nonferrous Met. Soc. China 32(2022) 3587−3595
Transactions of Nonferrous Metals Society of China
www.tnmsc.cn

Diffusion bonding of Ti−6Al−4V titanium alloy powder and solid by hot isostatic pressing

Yi XIAO, Li-hui LANG, Wen-cai XU, De-xin ZHANG

School of Mechanical Engineering and Automation, Beihang University, Beijing 100191, China

Received 22 September 2021; accepted 7 March 2022

Abstract: The Ti−6Al−4V (TC4) alloy powder and forged solid were diffusion bonded by hot isostatic pressing (HIP) to fabricate a powder−solid part. The microstructure of the powder−solid part was observed by scanning electron microscope (SEM). The microhardness and tensile tests were conducted to investigate the mechanical properties. The results showed that the powder compact was near-fully dense, and the powder/solid interface was tight and complete. The microhardness of the interface was higher than that of the powder compact and solid. The fractures of all powder−solid tensile specimens were on the solid side rather than at the interface, which indicated that a good interfacial strength was obtained. The tensile strength and elongation of the powder compact were higher than those of the solid. It is concluded that the HIP process can successfully fabricate high-quality Ti−6Al−4V powder−solid parts, which provides a novel near net shape technology for titanium alloys.

Key words: Ti−6Al−4V alloy; powder/solid interface; hot isostatic pressing; diffusion bonding; microstructure; mechanical properties

1 Introduction

Titanium alloys have been widely applied in the aerospace field due to their superior properties, including low density, high specific strength and stiffness, excellent corrosion resistance, and good creep resistance [1,2]. Ti−6Al−4V (TC4) is the most extensively used titanium alloy to manufacture aeronautical parts [3]. In recent years, the joining of titanium alloys to obtain hybrid structures with comprehensive properties has attracted much attention [4]. Welding technology is broadly employed to join titanium alloys, such as gas tungsten arc welding (GTAW) [5], electron beam welding (EBW) [6], laser beam welding (LBW) [7], friction welding [8], brazing [9], and diffusion bonding (DB) [10,11]. In recent years, diffusion bonding has been acknowledged as an attractive method to join titanium alloys [12]. There is no fusion zone, residual stress, or macroscopic deformation in the diffusion bonded joint [13].

Powder metallurgy (PM) methods enable the fabrication of compound components by combining solid materials with powder materials [14]. An innovative PM method is the hot isostatic pressing (HIP) which can provide sufficient heat and pressure to fully densify powders and make a diffusion bonding between the base materials simultaneously. Moreover, the joints obtained by hot isostatic pressing-diffusion bonding (HIP-DB) are good and reliable [15]. On the other hand, the manufacture of titanium alloy parts with complex shapes still has difficulties in actual applications. At present, casting [16] and machining [17] are the commonly used methods. Nevertheless, the cast titanium alloys and machined titanium alloys have some disadvantages [18]. The powder−solid forming via HIP, which enables the powder consolidation and diffusion bonding simultaneously,

Corresponding author: Yi XIAO, Tel/Fax: +86-17600142008, E-mail: xiaoyi0301@buaa.edu.cn
DOI: 10.1016/S1003-6326(22)66041-2

is put forward to realize the near net shape of titanium alloys. Due to the superior fluidity, spherical powders can facilitate assembly, obtain diverse diffusion bonding interfaces, and improve flexibility in the design of joints [19]. Titanium powders are also commonly used interlayers to join metals [20,21], composites [22,23], and ceramics [24]. As for the joining of the powder and solid, a two-step method has been put forward [25]. The powder is first consolidated by powder metallurgy methods, and then the obtained powder compact is diffusion bonded to the solid. Similarly, the two-step method can also be utilized to join dissimilar powders [26,27]. However, realizing powder consolidation and diffusion bonding simultaneously can save time and improve efficiency. For this purpose, the HIP diffusion bonding method to join powder and solid is proposed [28].

In this work, the Ti−6Al−4V powder and forged solid were diffusion bonded by the HIP process at 920 °C and 120 MPa for 2 h to fabricate the powder−solid part. The focus of this work was on the microstructure and mechanical properties of the obtained powder−solid part. The aim of this investigation is to explore a candidate near net shape technology for titanium alloys.

2 Experimental

2.1 Materials

The Ti−6Al−4V powder used in this study was prepared by plasma rotation electrode process (PREP), and the chemical composition is presented in Table 1. The powder particles are highly spherical with smooth surfaces, as shown in Fig. 1, which facilitates the flow and filling of powder. The average particle size of the powder is 123.58 μm. The Ti−6Al−4V solid used in this study was prepared by the forging process and processed into a cuboid. The 304 stainless steel capsule was employed, and the capsule was also processed into a cuboid with a wall thickness of 2 mm, whereas the upper cover was not welded. A hole was machined on the upper cover of the capsule for subsequent filling of powder.

Table 1 Chemical composition of Ti−6Al−4V powder (wt.%)

Al	V	Fe	C	N	H	O	Ti
6.6	3.65	0.02	0.02	0.01	0.001	0.15	Bal.

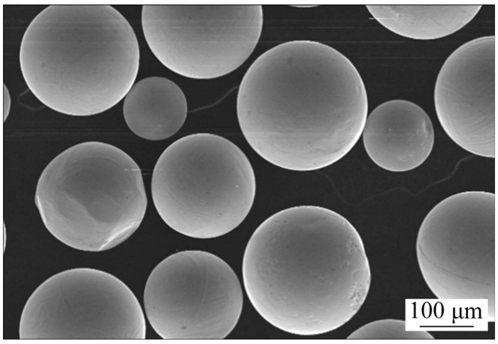

Fig. 1 Morphology of Ti−6Al−4V powder

2.2 Procedure

The oxide film on the surfaces of the Ti−6Al−4V solid was first ground by SiC papers. Then, the ultrasonic cleaning machine removed the oil on the surfaces of the solid and capsule with acetone. After drying, the solid was assembled into the capsule (see Fig. 2), and the upper cover of the capsule was welded. The Ti−6Al−4V powder was filled into the capsule through the hole on the upper cover. A vibration system was used to make the apparent density of the powder reach 65%. Subsequently, the capsule was degassed through the hole on the upper cover to remove the air by an FJ−620 molecular pump until the vacuum degree was 1.0×10^{-4} Pa. Finally, the HIP was carried out to fabricate the Ti−6Al−4V powder−solid part.

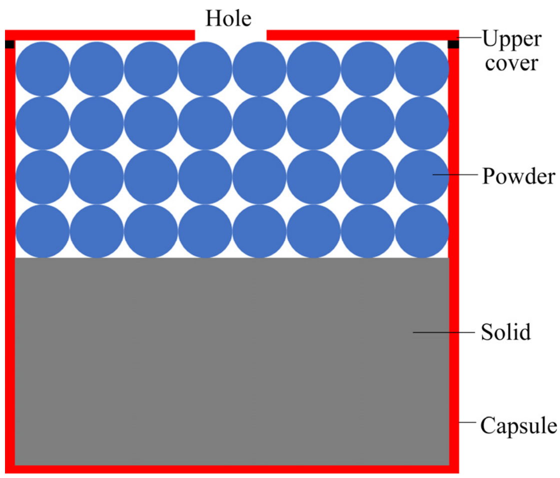

Fig. 2 Assembled samples

The Ti−6Al−4V powder−solid part prepared by HIP technology was obtained by simultaneously realizing powder metallurgy and diffusion bonding. The HIP parameters, including temperature, pressure, and holding time, have a great effect on the quality of powder metallurgy and diffusion bonding. Regarding the Ti−6Al−4V powder consolidation via HIP, detailed studies have been carried out previously [29], and the process parameters have been optimized [30]. In addition, CHEN et al [31] found that the compact prepared by HIP at 920 °C and 120 MPa for 2 h had the highest density and the best comprehensive mechanical properties. As for the Ti−6Al−4V diffusion bonding via HIP, ZHAO et al [32] studied the effects of process parameters on the microstructure and mechanical properties. They concluded that the good interface and bonding strength could be obtained when the holding temperature reached 800 °C under holding pressure of 120 MPa for 2 h. Moreover, HE et al [33] studied the influence of the process parameters on the diffusion bonding quality and shear strength of Ti−6Al−4V titanium alloy joints using orthogonal tests. They concluded that the optimal bonding temperature for Ti−6Al−4V titanium alloy was 920 °C. Therefore, in this study, the Ti−6Al−4V powder−solid part was fabricated under the HIP parameters of 920 °C, 120 MPa, and 2 h. Following HIP, the Ti−6Al−4V powder−solid part was obtained after removing the capsule.

2.3 Methods

The density of the Ti−6Al−4V hot isostatic pressed (HIPed) powder compact and solid was measured based on Archimedes' principle using an electron density meter (MDJ−600A). The microstructure and fracture morphology of the Ti−6Al−4V powder−solid part were observed using a scanning electron microscope (SEM, JSM6010). The metallographic specimen was cut from the powder−solid part by a wire cutting machine. Then, the metallographic specimen was ground, polished, and etched with Kroll's reagent (10 mL HF + 5 mL HNO_3 + 85 mL H_2O) before SEM observation. The Vickers hardness tester (FM800) was used to test the microhardness of the powder−solid part under a load of 1.96 N for 15 s. The tensile specimens were processed according to the GB/T 228.1—2010 standard for metallic material tensile testing. The geometry of tensile test specimens is shown in Fig. 3, and the gauge length of tensile specimens is 25 mm. The tensile tests were conducted on an electronic universal testing machine (CTM100G) with a speed of 2 mm/min at room temperature.

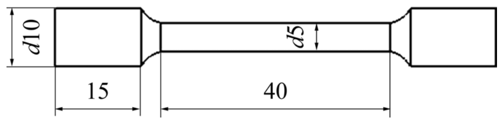

Fig. 3 Schematic diagram of tensile specimens (Unit: mm)

3 Results and discussion

3.1 Microstructure

The density was first measured, and five specimens were used to determine average density. The average densities of the Ti−6Al−4V HIPed powder compact and solid are 4.388 and 4.417 g/cm^3, respectively. Therefore, the relative density of the powder compact is 99.34%, which indicates that the powder compact is near-fully dense. Figure 4 shows the SEM micrographs of the Ti−6Al−4V powder−solid part. As shown in Fig. 4(a), no obvious internal voids or pores are observed in the powder compact region. The bonding between the powder particles is sound, and the prior particle boundary (PPB) is invisible. Therefore, the good metallurgical quality of the powder compact has been achieved by the HIP. The Ti−6Al−4V powder compact shows a duplex microstructure consisting of fine equiaxed grains and a lathlike structure. The equiaxed α phase is mainly distributed at the boundary of the prior powder particles. On the contrary, the lathlike α phase and the intercrystalline β phase are arranged alternately and mainly distributed in the interior of the prior powder particles. The reason is that the acicular martensite in the prior powder was transformed into the lathlike α phase and β phase at the HIP temperature. During the HIP process, the yield strength of the powder decreased at high temperatures, and the powder particles were extruded under high pressure. Hence, a large plastic deformation occurred at the boundary of the prior powder particles, which made the grains refined. In addition, a large amount of deformation energy was stored during the extrusion process. In the further heating and pressing process, dynamic recrystallization occurred, which led to the formation of equiaxed grains at the boundary of the prior powder particles. Unlike powder compact, the Ti−6Al−4V solid mainly shows a coarse lamellar structure, as illustrated in Fig. 4(b).

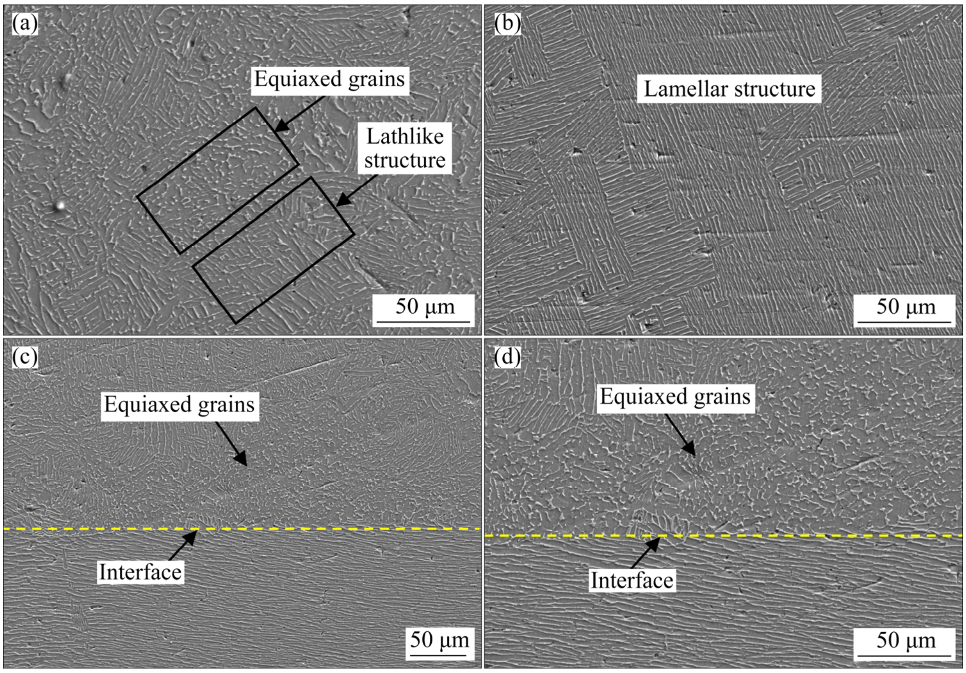

Fig. 4 SEM micrographs of powder−solid part: (a) Powder compact region; (b) Solid region; (c, d) Interface

As seen from Figs. 4(c, d), the Ti−6Al−4V powder/solid interface is tight and complete. No metallurgical defects such as voids, pores, and cracks are observed at the interface under low and high magnification observations of SEM. It is also believed that the HIP process can eliminate the defects [34]. The sound interface indicates that the good bonding between the powder and solid has been obtained by HIP as well. Additionally, the interface is relatively straight and regular, which indicates that the oxide film on the solid face is negligible because the oxide film can prevent the element diffusion [35]. There is no visible diffusion layer or gap at the interface, but obvious difference in microstructure type and gain size between the powder compact and solid can be observed. The diffusion layer does not exist because similar materials are selected in this study, and the diffusion layer is the feature when joining different materials by diffusion bonding. It is noticeable that the finer equiaxed grains were formed at the interface near the powder compact. This can be attributed to the severe extrusion deformation between the powder particles and the rigid solid under external pressure.

The HIP forming process of the Ti−6Al−4V powder−solid part included powder consolidation and powder−solid diffusion bonding. The mechanism of powder consolidation has been studied previously [36]. The mechanism of powder−solid diffusion bonding is analyzed in this work, as shown in Fig. 5. The formation of the powder/solid interface during the HIP process can be divided into the following stages. First, the powder particles were rearranged and approached the solid with the increase of pressure. Since the loose powder and the solid were in point contact, there were many voids between them at the interface. With the further increase of pressure, the normal stress on the powder surface increased. At the same time, the yield strength of the powder

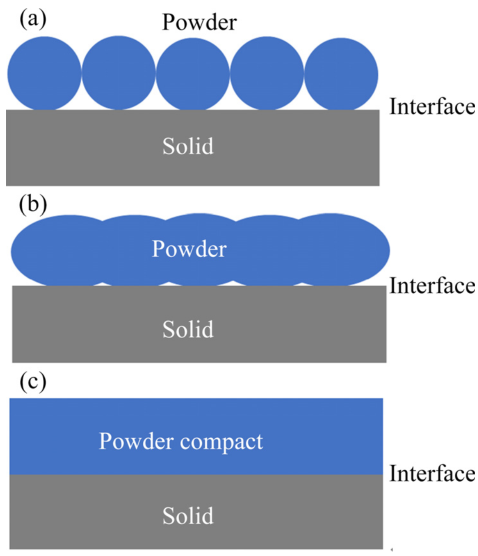

Fig. 5 Mechanism of powder−solid diffusion bonding: (a) Particle rearrangement; (b) Plastic deformation; (c) Element diffusion

decreased due to the increase in temperature. When the normal stress applied on the surface exceeded the yield strength of the powder, plastic deformation began to occur in the powder. In particular, the plastic deformation of the powder close to the large rigid solid was more severe. Therefore, the contact area between the powder and the solid increased. Moreover, the number and size of the voids at the interface decreased. When the powder was in close contact with the solid, the elements in the powder and the solid began to diffuse mutually. The diffusion distance and flux of the elements also increased when the temperature and holding time were further evaluated. Thus, the element diffusion between the powder and solid was sufficient, and the residual microvoids at the interface were eliminated. Furthermore, the creep of the powder also promoted the elimination of voids. Ultimately, a good powder/solid interface was formed, and the powder and solid were boned tightly. As described above, it can be concluded that the powder−solid diffusion bonding is realized by particle rearrangement, plastic deformation, and element diffusion under the effects of the HIP pressure, temperature, and holding time.

3.2 Mechanical properties

Microhardness and tensile strength are important indicators to evaluate mechanical properties. The microhardness of the Ti−6Al−4V powder compact, solid, and interface is given in Table 2. Five points for each position were measured to determine the average microhardness. It is presented that the interfacial microhardness is the highest, while the microhardness of the solid is the lowest. The reason for the microhardness variation is that the grains at the interface are the finest, while the grains in the solid are the coarsest. It is demonstrated that the powder−solid forming via HIP can improve the interfacial microhardness by grain refinement.

Table 2 Microhardness (HV) of specimens

Powder compact	Solid	Interface
319	289	384

The tensile specimens of the Ti−6Al−4V powder compact, solid, and powder−solid were prepared, as illustrated in Fig. 6. Three tensile specimens were tested to determine the average values of tensile properties. In particular, the interface was in the middle of the powder−solid tensile specimens, and the two sides of the interface are powder compact and solid, respectively. As presented in Fig. 6, the fracture surfaces of three kinds of specimens are all uneven with obvious necking, which indicates that the tensile fractures are ductile. An important phenomenon is that the fractures of all powder−solid tensile specimens are on the solid side rather than at the interface between the powder compact and solid. It is verified that the weakest area of the powder−solid tensile specimen is in the solid instead of at the powder/solid interface. Therefore, it is further implied that the powder/solid interface with high microhardness and strength can be obtained by the HIP process. In addition, the location of fractures also shows that the tensile strength of powder compact is higher than that of solid, which is related to the differences in microstructure between them. The type, content, distribution, and grain size of the phase have a significant effect on the properties of titanium alloys. The strength and plasticity of the equiaxed structure are better than those of the lamellar structure [37]. Moreover, the grain size of powder compact is finer than that of solid, and hence, the tensile strength is higher according to the fine-grain strengthening mechanism.

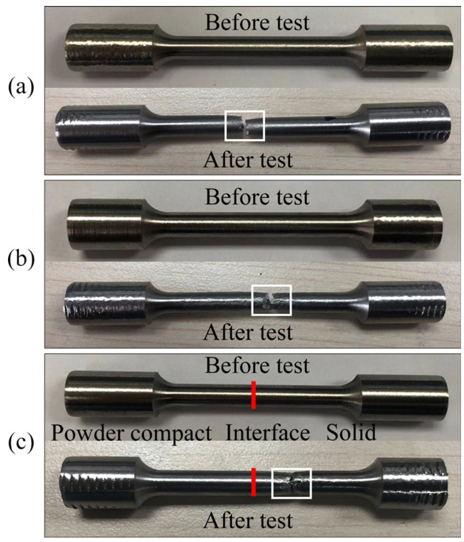

Fig. 6 Photos of tensile specimens before and after tensile tests: (a) Powder compact; (b) Solid; (c) Powder−solid

Table 3 presents the specific values of the tensile properties for three kinds of specimens. The tensile strength and elongation of the powder compact specimens are 13% and 28% higher than those of the solid specimens, respectively. As expected, the tensile strength of the powder−solid specimens is similar to that of the solid specimens because the powder−solid tensile specimens fail on the solid side. However, the elongation of the powder−solid specimens is slightly lower than that of the solid specimens. The reason is that the other side of the powder−solid specimens is powder compact with higher tensile strength.

Table 3 Tensile properties of specimens

Specimen	Tensile strength/MPa	Elongation/%
Powder compact	939.1	20.1
Solid	830.9	15.7
Powder−solid	827.1	12.1

3.3 Fractography

The fracture surfaces of the tensile specimens were observed to further analyze the fracture mechanism. From Figs. 7(a, b), the fracture surface of the Ti−6Al−4V powder compact is uneven and fibrous. A mass of dimples and tearing ridges are found on the fracture surface, as shown in Figs. 7(c, d). The large and deep dimples show that the tensile fracture exhibits excellent ductility. The noticeable tearing ridges indicate that the plastic deformation is sufficient during the tensile process. These features are in good agreement with the tensile test results, which present the excellent strength and elongation of the powder compact. It is speculated that the fracture process of powder compact is the coalescence of microvoids and the formation and propagation of cracks. First, microvoids occurred when the tensile stress increased. Then, the microvoids gradually coalesced to form cracks under large plastic deformation. Finally, the cracks propagated until the tensile specimens failed.

The fracture surfaces of the Ti−6Al−4V solid are also uneven, as shown in Fig. 8(a). The dimples are observed on the fracture surface in Fig. 8(b), whereas the dimples are smaller and shallower than those of the powder compact. Moreover, there are some cleavage steps on the fracture surfaces in Fig. 8(c), which indicates that the brittle fracture also occurred. Therefore, although the tensile fracture of solid mainly exhibits ductility, it still has brittle characteristics. It is evident that the plasticity of the solid is not as good as that of the powder compact, which is in good accordance with the tensile test results. It is speculated from the cleavage facets (Fig. 8(d)) that the fracture process of solid is transgranular. The microvoids first occurred at the boundaries of lamellar grains, and then the microvoids grew and coalesced to form

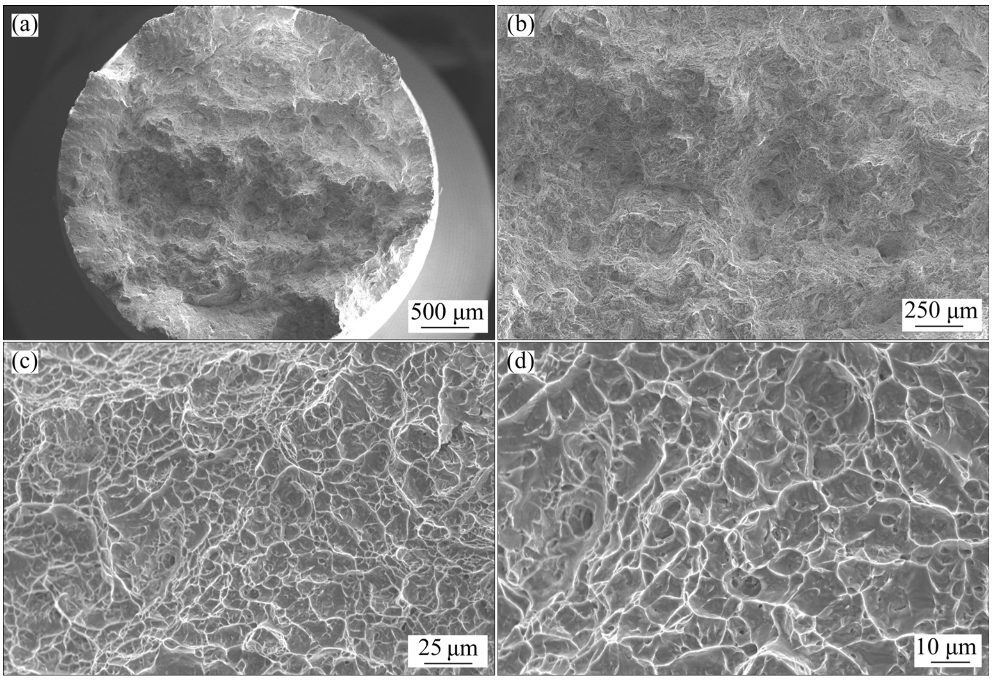

Fig. 7 SEM micrographs of tensile fracture for powder compact: (a) Morphology of overall fracture; (b) Magnified image of (b); (c) Morphology of dimples; (d) Magnified image of (c)

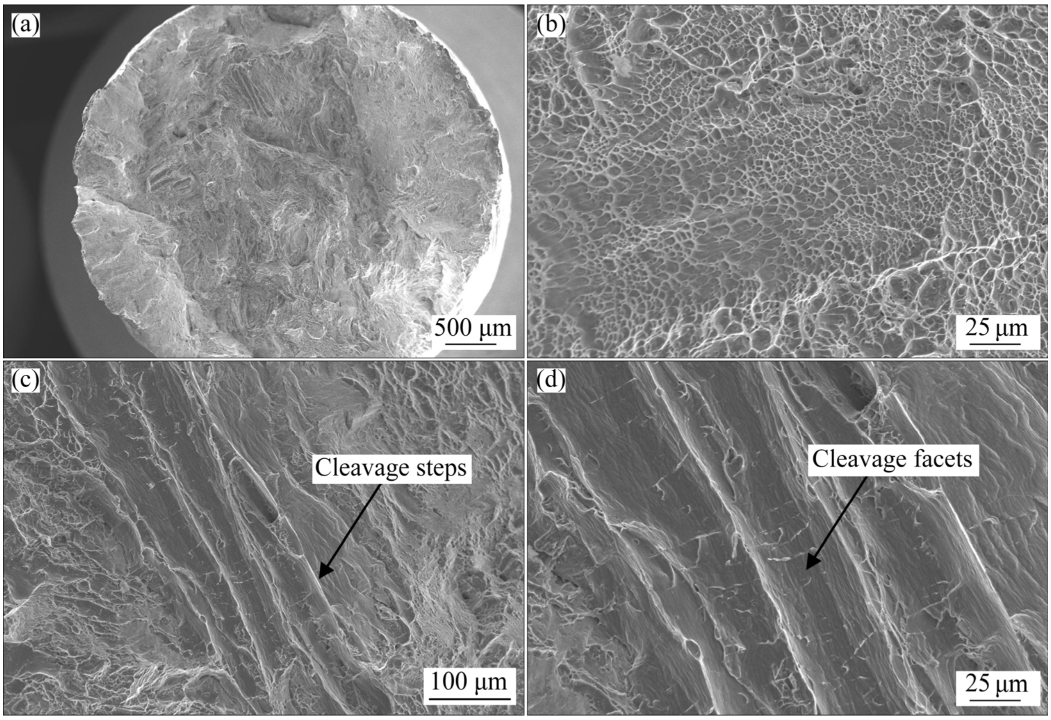

Fig. 8 SEM micrographs of tensile fracture for solid: (a) Morphology of overall fracture; (b) Morphology of dimples; (c) Morphology of cleavage characteristics; (d) Magnified image of (c)

cracks. The cracks propagated along the direction of cleavage steps, thus resulting in transgranular fracture. As for the fracture surfaces of the powder−solid specimens, the observed morphology is consistent with the fracture surfaces of the solid as the fractures are on the solid side.

4 Conclusions

(1) The Ti−6Al−4V powder and forged solid were diffusion bonded successfully by HIP under the process parameters of 920 °C, 120 MPa, and 2 h, and a high-quality powder−solid part was obtained. The powder compact is near-fully dense with no obvious internal voids or pores. The microstructure of the powder compact is composed of the equiaxed α phase and lathlike α phase, whereas the microstructure of the solid is composed of the lamellar α phase. Particularly, the finer equiaxed grains are formed at the interface.

(2) The powder/solid interface is tight, straight, and free of defects. The diffusion layer is invisible at the interface, but the powder compact and solid can be distinguished by different phases. It is analyzed that the good interface is obtained by particle rearrangement, plastic deformation, and element diffusion.

(3) The average microhardness of the Ti−6Al−4V powder/solid interface is the highest due to the finest grains. The tensile strength and elongation of the powder compact are 13% and 28% higher than those of the solid, respectively. All powder−solid tensile specimens fail on the solid side rather than at the interface, indicating that the tensile strength of the interface is higher than that of the solid.

(4) The tensile fracture of the powder compact exhibits more excellent ductility than that of the solid. The dimples on the fracture surfaces of the powder compact are large and deep, and the tearing edges are obvious. On the contrary, there are some cleavage characteristics on the fracture surfaces of the solid. The fracture morphology of the powder−solid specimens is consistent with that of the solid since the fractures are on the solid side.

Acknowledgments

The authors are grateful for the financial support from the National Natural Science Foundation of China (No. 51675029).

References

[1] LI Hong, LI Miao-quan, LIU Hong-bin, ZHANG Chao. Effect of grain size of primary α phase on bonding interface characteristic and mechanical property of press bonded Ti−6Al−4V alloy [J]. Transactions of Nonferrous Metals Society of China, 2016, 26(1): 93−99.

[2] ATIEH A M, KHAN T I. Effect of process parameters on semi-solid TLP bonding of Ti−6Al−4V to Mg−AZ31 [J]. Journal of Materials Science, 2013, 48(19): 6737−6745.

[3] ARTAZA T, SUAREZ A, VEIGA F, BRACERAS I, TABERNERO I, LARRANAGA O, LAMIKIZ A. Wire arc additive manufacturing Ti6Al4V aeronautical parts using plasma arc welding: Analysis of heat-treatment processes in different atmospheres [J]. Journal of Materials Research and Technology, 2020, 9(6): 15454−15466.

[4] THIRUNAVUKARASU G, CHATTERJEE S, KUNDU S. Scope for improved properties of dissimilar joints of ferrous and non-ferrous metals [J]. Transactions of Nonferrous Metals Society of China, 2017, 27(7): 1517−1529.

[5] MUTH T R, YAMAMOTO Y, FREDERICK D A, CONTESCU C I, CHEN W, LIM Y C, PETER W H, FENG Z. Causal factors of weld porosity in gas tungsten arc welding of powder-metallurgy-produced titanium alloys [J]. JOM, 2013, 65(5): 643−651.

[6] BOYANGIN E N, PEREVALOVA O B, PANIN A V, MARTYNOV S A. The effect of electron beam welding on the microstructure and microhardness of 3D-printed products from titanium alloy Ti−6Al−4V [J]. Physics of Metals and Metallography, 2021, 122(2): 141−147.

[7] SAHOO S K, BISHOYI B, MOHANTY U K, SAHOO S K, SAHU J, BATHE R N. Effect of laser beam welding on microstructure and mechanical properties of commercially pure titanium [J]. Transactions of the Indian Institute of Metals, 2017, 70(7): 1817−1825.

[8] WANG Xin-yu, LI Wen-ya, YE Qing, YANG Xia-wei, MA Tie-jun, VAIRIS A. Linear friction welding of a beta titanium alloy: Experimental investigations on microstructure evolution and mechanical properties [J]. Science and Technology of Welding and Joining, 2020, 25(8): 625−636.

[9] MARINHO C, TOPTAN F, GUEDES A, ALVES A C. Electrochemical response of Ti joints vacuum brazed with TiCuNi, AgCu, and Ag fillers [J]. Transactions of Nonferrous Metals Society of China, 2021, 31(4): 999−1011.

[10] LIN Peng, XI Xian-zheng, ZHAO Wen-kai, YANG Rui-hong, LIN Fei, CUI Xiao-lei, LIU Gang. Microstructure and mechanical properties of Ti−6Al−4V/Ti−22Al−25Nb joint formed by diffusion bonding [J]. Transactions of Nonferrous Metals Society of China, 2021, 31(5): 1339−1349.

[11] FERGUSON B, RAMULU M. Surface tracking of diffusion bonding void closure and its application to titanium alloys [J]. International Journal of Material Forming, 2020, 13(4): 517−531.

[12] BALASUBRAMANIAN M. Development of processing windows for diffusion bonding of Ti−6Al−4V titanium alloy and 304 stainless steel with silver as intermediate layer [J]. Transactions of Nonferrous Metals Society of China, 2015, 25(9): 2932−2938.

[13] LI Hong, ZHANG Chao, LIU Hong-bin, LI Miao-quan. Bonding interface characteristic and shear strength of diffusion bonded Ti-17 titanium alloy [J]. Transactions of Nonferrous Metals Society of China, 2015, 25(1): 80−87.

[14] LINDWALL G, FLYG J, FRISK K, SANDBERG O. Experimental and theoretical investigations of hot isostatically pressed-produced stainless steel/high alloy tool steel compound materials [J]. Metallurgical and Materials Transactions A, 2011, 42(5): 1165−1172.

[15] XIAO Yi, LANG Li-hui, XU Wen-cai. Microstructure and mechanical properties of CuAgZn/GH909 diffusion bonded joint fabricated by hot isostatic pressing [J]. Transactions of Nonferrous Metals Society of China, 2021, 31(2): 475−484.

[16] XIAO Shu-long, CHEN Yu-yong, ZHU Hong-yan, TIAN Jing, WU Bao-chang. Recent advances on precision casting of large thin wall complex castings of titanium alloys [J]. Rare Metal Materials and Engineering, 2006, 35(5): 678−681. (in Chinese)

[17] REVURU R S, POSINASETTI N R, RAMANA V V S N, AMRITA M. Application of cutting fluids in machining of titanium alloys-a review [J]. The International Journal of Advanced Manufacturing Technology, 2017, 91(5/6/7/8): 2477−2498.

[18] BANERJEE D, WILLIAMS J C. Perspectives on titanium science and technology [J]. Acta Materialia, 2013, 61(3): 844−879.

[19] LANG Ze-bao, WANG Liang, ZHANG Xu-hu. HIP diffusion bonding of P/M titanium alloy Ti−6Al−4V and stainless steel 1Cr18Ni9Ti [J]. Transactions of Nonferrous Metals Society of China, 2007, 17(S1): s79−s83.

[20] SALMALIYAN M, SHAMANIAN M. Effect of Ti powders addition on mechanical and metallurgical properties of IN718/BNi-2/316L diffusion couple [J]. Transactions of the Indian Institute of Metals, 2020, 73(5): 1157−1169.

[21] CHEN Hong-yu, LUO Lai-ma, ZHANG Jun, ZAN Xiang, ZHU Xiao-yong, LUO Guang-nan, WU Yu-cheng. Investigation on W/Fe diffusion bonding using Ti foil and Ti powder interlayer by SPS [J]. Journal of Nuclear Materials, 2015, 467: 566−571.

[22] WANG B, JIANG S S, ZHANG K F. Pulse current auxiliary TLP diffusion bonding of SiC_p/2024Al composite sheet using mixed Al−Cu−Ti powder interlayer [J]. The International Journal of Advanced Manufacturing Technology, 2013, 65(9/10/11/12): 1779−1784.

[23] WANG Bo, JIANG Shao-song, ZHANG Kai-feng. Effects of pulse current on transient liquid phase (TLP) diffusion bonding of SiC_p/2024Al composites sheet using mixed Al, Cu, and Ti powder interlayer [J]. Metallurgical and Materials Transactions A, 2012, 43(9): 3039−3042.

[24] WU Li-xiang, GUO Wei-ming, NIU Wen-bin, LIN Rui-lin, SUN Shi-kuan, XUE Jia-xiang, LIN Hua-tay. Pressureless joining of SiC ceramics at low temperature [J]. Ceramics International, 2019, 45(5): 6556−6559.

[25] XUE Z, YANG Q, GU L, HAO X, REN Y, GENG Y. Diffusion bonding of TiAl based alloy to Ti−6Al−4V alloy using amorphous interlayer [J]. Materialwissenschaft und Werkstofftechnik, 2015, 46(1): 40−46.

[26] PRIKHODKO S V, SAVVAKIN D G, MARKOVSKY P E,

STASUK O O, PENNEY J, SHIRZADI A A, DAVIES P D, DAVIES H M. Diffusion bonding of TiC or TiB reinforced Ti−6Al−4V matrix composites to conventional Ti−6Al−4V alloy [J]. Science and Technology of Welding and Joining, 2020, 25(6): 518−524.

[27] CHENG Min, YU Bing-bing, GUO Rui-peng, SHI Xiao-hui, XU Lei, QIAO Jun-wei, YANG Rui. Electron beam welding of a novel near alpha high temperature titanium alloy powder compact: effect of post-welding heat treatment on tensile properties [J]. Journal of Materials Research and Technology, 2021, 10: 153−163.

[28] CAI Chao, GAO Xiang-yun, TENG Qing, LI Ming, PAN Kun-kun, SONG Bo, YAN Chun-ze, WEI Qing-song, SHI Yu-sheng. A novel hybrid selective laser melting/hot isostatic pressing of near-net shaped Ti−6Al−4V alloy using an in-situ tooling: Interfacial microstructure evolution and enhanced mechanical properties [J]. Materials Science and Engineering A, 2018, 717: 95−104.

[29] XUE Y, LANG L H, BU G L, LI L. Densification modeling of titanium alloy powder during hot isostatic pressing [J]. Science of Sintering, 2011, 43(3): 247−260.

[30] LANG Li-hui, BU Guo-liang, XUE Yong, ZHANG Dong-xing. Determine key parameters of simulation constitutive and process optimization for titanium alloy (Ti−6Al−4V) hot isostatic pressing [J]. Journal of Plasticity Engineering, 2011, 18(4): 34−38. (in Chinese)

[31] CHEN Jian-hong, XIAO Le, CHEN Yong-qing, YAN Ying-jie, CAO Rui. The effect of hot isostatic pressing temperature on the microstructure and tensile properties of TC4 alloy [J]. Journal of Lanzhou University of Technology, 2021, 47(1): 1−4. (in Chinese)

[32] ZHAO Bing, LIAO Jin-hua, HAN Xiu-quan, HOU Hong-liang, LI Zhi-qiang. Manufacturing method and mechanical property of titanium hollow structure based on HIP process [J]. Aeronautical Manufacturing Technology, 2018, 61(18): 36−42. (in Chinese)

[33] HE Chen-jia, CHEN Ming-he, XIE Lan-sheng. Study on diffusion bonding process of TC4 titanium alloy [J]. Hot Working Technology, 2017, 46(17): 64−68. (in Chinese)

[34] WATKINS I T, DAVIES H M, STANNERS O G, MARCHISIO S. Powder interlayer bonding of geometrically complex Ti−6Al−4V parts [J]. The International Journal of Advanced Manufacturing Technology, 2020, 106(9/10): 3629−3639.

[35] SANG Chang-cheng, CAI Xiao-ping, ZHU Lu, REN Xuan-ru, NIU Gao, WANG Xiao-hong, FENG Pei-zhong. Dissimilar metal joining of Ti and Ni using Ti−Al powder interlayer via rapid thermal explosion method [J]. Journal of Materials Engineering and Performance, 2020, 29(11): 7239−7249.

[36] HUANG Xi-na, LANG Li-hui, WANG Gang, ALEXANDROV S. Effect of powder size on microstructure and mechanical properties of 2A12Al compacts fabricated by hot isostatic pressing [J]. Advances in Materials Science and Engineering, 2018: 1989754.

[37] KIM Y, SONG Y B, LEE S H. Microstructure and intermediate-temperature mechanical properties of powder metallurgy Ti−6Al−4V alloy prepared by the prealloyed approach [J]. Journal of Alloys and Compounds, 2015, 637: 234−241.

Ti−6Al−4V 合金粉末与固体热等静压扩散连接

肖 毅，郎利辉，徐文才，张德鑫

北京航空航天大学 机械工程及自动化学院，北京 100191

摘 要：通过热等静压(HIP)扩散连接 Ti−6Al−4V(TC4)合金粉末和锻件固体成形粉−固零件。利用扫描电镜(SEM)观察粉−固零件的显微组织，并开展显微硬度和拉伸实验研究其力学性能。结果表明，粉−固零件中粉末压块接近全致密，粉/固界面紧密且完整。界面的显微硬度高于粉末压块和固体的。粉−固拉伸试样都在固体一侧断裂而不是在界面处，这表明获得良好的界面强度。粉末压块的抗拉强度和伸长率都高于固体的。由此得出，热等静压工艺可以成功成形高质量的 Ti−6Al−4V 粉−固零件，这能为钛合金提供一种新型近净成形技术。

关键词：Ti−6Al−4V 合金；粉/固界面；热等静压；扩散连接；显微组织；力学性能

(Edited by Bing YANG)